

## Method of photodynamic inactivation of viruses in air

© I.M. Belousova,<sup>1</sup> V.M. Kiselev,<sup>2</sup> I.V. Bagrov,<sup>2</sup> T.D. Murav'eva,<sup>2</sup> A.M. Starodubtsev,<sup>2</sup> T.K. Krisko,<sup>1</sup>  
O.S. Zhitenev,<sup>1</sup> V.V. Zarubaev,<sup>3</sup> A.A. Shtro<sup>4</sup>

<sup>1</sup> Vavilov State Optical Institute, St. Petersburg, Russia

<sup>2</sup> Vavilov State Optical Institute, St. Petersburg, Russia

<sup>3</sup> Saint-Petersburg Pasteur Institute, Saint-Petersburg, Russia

<sup>4</sup> Smorodintsev Research Institute of Influenza (a Russian Ministry of Health federal institution), St. Petersburg, Russia  
e-mail: belousova.i.m@gmail.com

Received December 29, 2021

Revised February 28, 2022

Accepted March 3, 2022

The photodynamic inactivation of viruses by a microporous photocatalytic element made of copper or copper alloy is the very method of ensuring biosafety that the article is about. Based on this method, encouraging results of virological studies (using the influenza virus as a test) were obtained as well as the equipment solving the strategic task of antiviral (influenza, COVID-19, etc.) disinfecting and sterilizing of confined spaces air, including air of medical premises, was developed.

**Keywords:** air sterilization, copper, microporous membrane, influenza virus, singlet oxygen.

DOI: 10.21883/TP.2022.07.54489.330-21

### Introduction

Biological safety of mankind is challenging issue of the modern age, including both life environment safety, primarily the safety of air, water and surrounding items, and medical treatment agents based on biological liquids, for example, donated blood and saline solution.

Respiratory diseases constitute a major medical and social problem and cause annual epidemics involving a large part of human population. The most widespread infection in this group is flu, with up to 15% world population having it annually, and for some hundreds of thousands people this disease is fatal [1]. The major respiratory infections in terms of fatalities for the last century included COVID-19, Hong Kong flu that caused one four million fatalities during 1968–1970 [2] and Spanish flu that claim the lives of about 50 million people during 1918–1920 [3].

High mutation accumulation rate enables the virus to avoid host immune system leading to the need to change vaccine composition to protect population during the current epidemic season, for example, for influenza virus this shall be done annually [4].

One of the important respiratory infection prevention methods include air disinfection measures in the indoor air where virus particles may be contained.

During long period, generally oxidation processes using chlorine and other chemical disinfectants have been applied for water decontamination and disinfection. However, the use of chemicals for air decontamination results in unnecessary growth of chemical load on human body, because disinfectants are applied directly to the human habitat as opposed to industrial chemical contaminations. Therefore, more sparing physical disinfection methods come to the fore in the air decontamination applications [5].

Such methods currently include: filtration, ozone treatment, UV irradiation, photocatalysis, electrical discharge, plasma.

The air decontamination methods and techniques listed above are generally proprietary and implemented in various instruments and devices, however, each of them has disadvantages.

The most evident system is an air filtration unit with HEPA filters [6] consisting of 0.5 to 2  $\mu\text{m}$  fiberglass microfiber system. These filters are capable of entrapping pathogens and particles from 0.003  $\mu\text{m}$  with efficiency of 99.5%. Disadvantage of these devices is in accumulation of viable viruses precipitated on filters and their potential „burst release“ during filter exchange resulting in personnel and room contamination.

Ultraviolet emission of antibacterial mercury-vapor lamps with wavelength range 205–315 nm ( $\lambda = 254$  nm emission is the most efficient), e.g. as in the device described in patent [7] are widely used for indoor air decontamination. However, the presence of UV emission results in the accumulation of harmful substances such as ozone and nitrous oxide exerting poisoning and damaging action of human body [8]. Such devices is reasonably to use in well ventilated areas without people inside them.

Air decontamination using ozone systems [9] has high oxidizing capacity and efficiently destroys pathogenic microbial flora. In addition, ozone concentrations required for efficient decontamination and created by the system exceed the specified maximum allowable concentrations (MAC) (single — 0.16  $\text{mg}/\text{m}^3$  and daily average — 0.03  $\text{mg}/\text{m}^3$ ) [10], therefore, such systems may be only used in the absence of people.

Method and devices based on pathogen inactivation using corona discharge shall be also addressed [11]. Heteropolar corona discharges are produced in the inactivation zone and

microorganisms are exposed to constant electric fields with drastically changing strength and gradient and to ions with opposite signs resulting in full destruction or electroporation (formation of membrane pores) of microorganisms. Disadvantage of this method is that high electric field strengths exceeding the air discharge strength are required for microorganism destruction or electroporation [5]. Moreover, the presence of high voltages requires instrument operation by highly skilled personnel and is unsafe in living environment.

From our point of view, photocatalytic air decontamination method and systems based on it are of utmost interest. An electron-hole pair is formed in the photocatalyst semiconductor when exposed to absorbed emission. The electron and hole on the semiconductor surface may react with oxygen molecules and other impurities absorbed on the same surface producing reactive oxidant forms, including hydroxyl radical  $\text{OH}^\bullet$ , superoxide anion radical  $\text{O}_2^{\bullet-}$ , and singlet oxygen obtained as result of interaction between  $\text{O}_2^{\bullet-}$  and hole ( $\text{h}^+$ ) [12,13].

These reactive oxidant forms have effective impact on pathogens. Thus, their anti-inflammatory effect investigated during antibacterial and antimycotic photo activated therapy was compared with the therapeutic benefit of traditional antibacterial and antifungal methods [14], and the antiviral research review has shown their ability to inactivate both enveloped and non-enveloped DNA and RNA viruses and suggesting that even SARS-CoV-2 may be inactivated [15].

Currently, air decontamination photocatalyst is generally implemented on the titanium dioxide basis. Thus, in Tiokraft system [16], titanium dioxide is applied directly on the lamp surface. Photocatalytic element is illuminated by UV emission sources ( $\lambda = 320\text{--}405\text{ nm}$ ), because  $\text{TiO}_2$  semiconductor band gap edge corresponds to  $\lambda = 388\text{ nm}$ .

Titanium dioxide based photocatalytic devices are being improved extensively [17], because their benefit is in that the reactive oxidants produced by photocatalysis are capable of destroying any type of pathogenic microorganisms.

The use of UV emission for photocatalyst activation is a serious disadvantage of titanium dioxide photocatalytic devices. Even when ozoneless antibacterial lamps are used, ozone formation still takes place though in less concentration. This disadvantage limits the use of such oxidating systems in occupied rooms. The use of light rays could avoid this problem, however, it is known that titanium dioxide photocatalytic element performance is reduced dramatically in this case. Inadequate titanium dioxide coating strength is also an additional disadvantage of this device, which in some cases results in titanium dioxide nanoparticle shedding from the carrier and release into air. For this it should be considered that a growing number of evidences that exposure to titanium dioxide nanoparticles ( $\text{TiO}_2$  NP) may be harmful [18], in particular during long-term exposure.  $\text{TiO}_2$  nanoparticles cause endothelial cell dysfunction and glial cell damage. Inhaled particles may cause systemic impacts and may move from lung and penetrate into the main biological structures which, in turn, may cause malfunction [19].

Recent investigations have also shown that  $\text{TiO}_2$  NP may cause cellular toxicity effects in heart tissue [20]. Toxic effects of  $\text{TiO}_2$  NP were also observed in blood system cells.

The purpose of the research herein was to develop a safe photo activated air decontamination method in enclosed rooms and ventilation systems without using high voltages and UV emission avoiding air ionization and ozonizing, as well as a device based on this method and having verified antiviral activity. The proposed method is based on the application of two physical methods of destructive effect on bacteria, viruses and other pathogen microorganisms contained in the air to be treated. The first method is based on the use of metals having antibacterial and antiviral action and nontoxic for body such as silver, zinc, copper or their mixtures, as disinfecting materials. The second method is based on oxidizing properties of the photocatalytic element made using these metals. These two methods efficiently supplement each other because a well known „contact form“ of pathogen inactivation on the surface of these metals is enhanced due to photocatalytic formation of reactive oxygen intermediates on the same surfaces exposed to visible light. This fact, together with „contact killing“ of bacteria and viruses, also indicates rather high photocatalytic activity of these metals [21]. Actually, copper as opposed to silver and zinc demonstrates quicker and higher efficiency against bacteria, viruses and other pathogens which have close contact with the surface in indoor ambient conditions which increases its application range. Therefore, copper or bronze, as a copper alloy, were used as photocatalytic element in the air decontamination device developed using the proposed method [22].

## 1. Copper-based photocatalytic element

Unique copper properties, in particular high oligodynamic effect („contact killing“) on bacteria, viruses and fungi, have long ago attracted attention of researchers to the investigation of copper as antibacterial, antifungal and antiviral material [23,24]. Although the oligodynamic effect of copper was well known from as early as ancient times, and currently growing interest in it is displayed again due to potential use of copper as antibacterial material in medical facilities. Together with pure copper, copper alloys may be used, for example, bronze, but its antiviral activity depends on copper percentage in alloy that shall be not lower than 85–90%. Norovirus destruction on surfaces made of copper alloys was described in [25]. Human coronavirus 229E was also quickly inactivated in some copper alloys (in a few minutes) [21], and Cu/Zn alloy was very effective with lower copper concentrations. Copper impact destroyed viral genomes and inadvertently influenced the virus morphology. Cu(I) and Cu(II) were responsible for pathogen inactivation which was enhanced by illumination due to formation of reactive oxygen intermediates on alloy surfaces [21]. This shows, as has been noted above, high photocatalytic activity of copper, therefore copper alloy

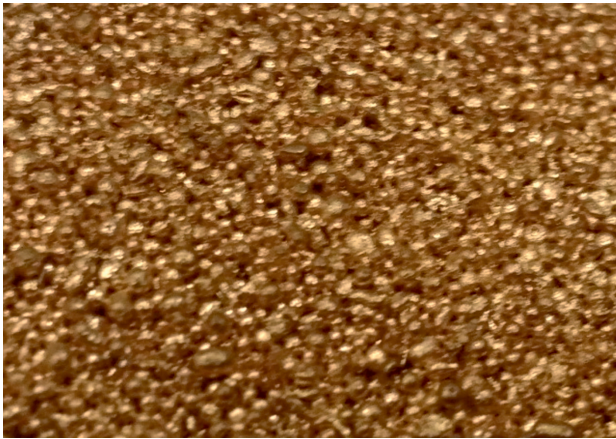


**Figure 1.** Bronze microporous membrane (top view).

surfaces may be used in public spaces and during any public events in order to help in reducing virus transfer from contaminated surfaces and to protect health.

Considering the above, we offered copper and copper to be used in the photocatalytic element constituting the basis of a safe photo activated air decontamination method in closed rooms and ventilation systems. Air decontamination unit developed using this principle has reliably proved its antiviral activity [22].

In the proposed air purification and sterilization unit, the photocatalytic element consists of a copper or bronze microporous membrane (Figure 1) illuminated by visible light through which the air to be purified is purged. Porous structure of a photocatalytic element facilitates the photo activated property performance of copper surface during pathogen inactivation in the air to be decontaminated, because this significantly increases the surface area to be irradiated (contact area). When illuminated with visible light from a LED source, a 3 mm microporous membrane uses its whole volume because high reflectivity of copper surface (60–70% on average) facilitates deep light penetration into the volume during multiple light reflections from the pore surfaces. As a result, it demonstrates high pathogen destruction performance. Deep penetration of the LED source light into the microporous membrane volume is confirmed by direct observation of visible light emission at the membrane outlet. The authors did not evaluate the optimum thickness of such microporous plates. This has yet to be done during future modernization.

Additional benefits of the proposed method compared with titanium dioxide photocatalytic elements include increased structural strength of the photocatalytic elements, since there is no coating shedding as is the case with titanium dioxide, because the copper containing element is solid.

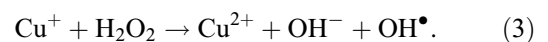
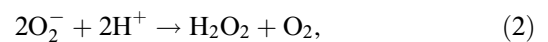
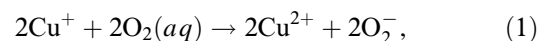
## 2. Copper-based photocatalytic element operation mechanisms

Two basic types of antibacterial, antifungal and antiviral action mechanisms of copper and copper alloys are well known: contact and photocatalytic. They are divided into two groups: mechanisms acting without illumination and mechanisms making their contribution with illumination of copper containing elements.

### 2.1. Mechanisms requiring no illumination

Oligodynamic effect or „contact killing“ — direct impact of copper ions on viruses, diffusion into the biological object from the media interface [23], is the main virus inactivation mechanism on 100% copper surfaces.

Generation of destructive oxygen radicals with the involvement of various particles absorbed on the copper surface (by molecular oxygen or viral envelope) is another pathogen inactivation mechanism playing an important role on the copper alloy surfaces [21]:



### 2.2. Mechanisms requiring illumination

Chemical composition of dry copper surfaces in ambient conditions generally also contains CuO and Cu<sub>2</sub>O with high prevailing content of Cu<sub>2</sub>O compared with CuO.

Photocatalytic processes on the copper surface containing copper oxides are similar to photocatalytic processes on TiO<sub>2</sub> surface [12,13,26] (Figure 2).

For copper oxide photocatalysis with illumination of copper surfaces by visible light (band gap of CuO is 1.3–2.1 eV, and of Cu<sub>2</sub>O is 2.1–2.6 eV), oxygen radicals are formed again with participation of

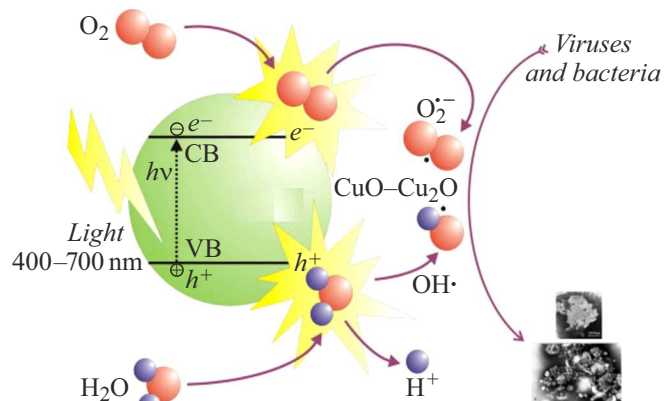
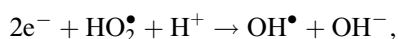
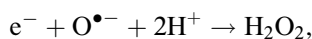
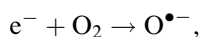
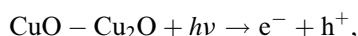
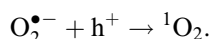


**Figure 2.** Diagram of photocatalysis on copper oxides.

particles absorbed on the copper surface (by molecular oxygen or viral envelope) [26]:



which can show excellent antibacterial and antiviral performance. In this case,  $\text{Cu}_2\text{O}$  has the same activity in pathogen destruction as pure copper, therefore, the copper surface retains its antimicrobial and antiviral properties even after oxide formation [26].  $\text{CuO}$  has somehow lower performance than pure copper, but its role is insignificant under prevailing influence of  $\text{Cu}_2\text{O}$ . During photocatalysis, singlet oxygen is also formed as a result of superoxide anion radical interaction with hole [12,13]:



It should be noted that singlet oxygen can occur not only as a result of photocatalysis, but also as a result of direct excitation of molecular oxygen absorbed on the copper surface [27].

### 3. Direct excitation of singlet oxygen on the photocatalytic copper alloy element surface

In experiments with copper membrane surface (diameter 30 mm, thickness 3 mm pore diameter 0.5 to 20  $\mu\text{m}$ ) by LED matrix visible light, we observed single oxygen

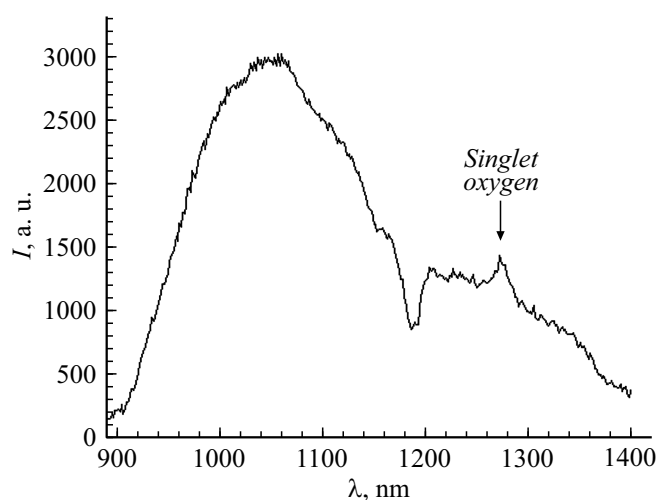


**Figure 3.** Singlet oxygen luminescence at transition  ${}^1\Delta_g\text{O}_2 \rightarrow {}^3\Sigma_g\text{O}_2$  ( $\lambda = 1270$  nm) during copper surface exposure to 405 nm light.

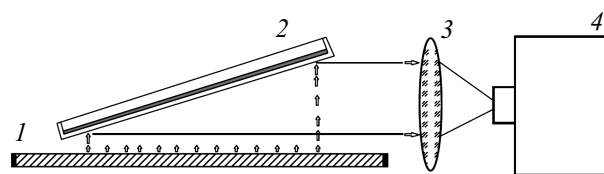


**Figure 4.** Diagram of the experiment: 1 — LED matrix 26 × 26 mm, 2 — Cu film on 30 mm diameter glass, 3 — lens, 4 — SDH-IV spectrometer.

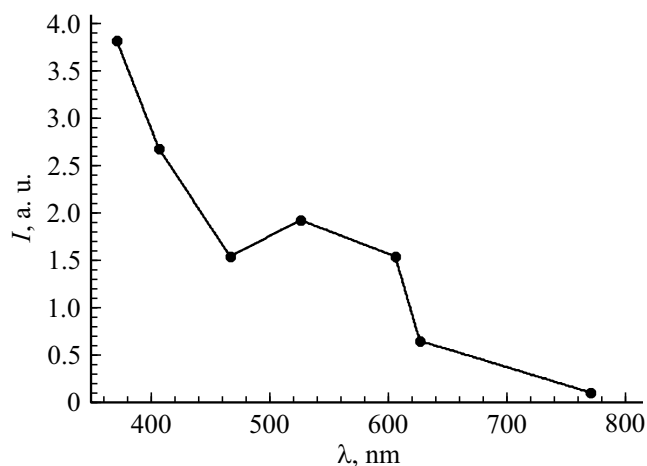


**Figure 5.** Spectral dependence of oxygen phosphorescence with direct excitation by LED matrix light.

luminescence. Figure 3 shows singlet oxygen luminescence when copper surface is exposed to  $\lambda_m = 405$  nm and  $\Delta\lambda_{0.5} \approx 20$  nm LED matrix light. 26 × 26 mm LED matrix light flux density was 0.6 W/cm<sup>2</sup>, exposure time was 12 s. The experimental setup is shown in Fig. 4. Singlet oxygen luminescence performance investigation used singlet oxygen luminescence recording method in IR region at transition  ${}^1\Delta_g\text{O}_2 - {}^3\Sigma_g\text{O}_2$  ( $\lambda = 1270$  nm) using „Slar Laser Systems“ (Belarus) SDH-IV IR spectrometer with Hamamatsu InGaAs receiving line (Japan). This instrument enables reliable recording of singlet oxygen phosphorescence spectrum simultaneously with background luminescent irradiation of copper surface, of phosphorescence intensity to compare the test samples with each other. Spectral resolution limit in the test range 1065–1330 nm does not exceed 1.3 nm. The luminescent singlet oxygen is observed from the whole exposed copper surface.

Supposed singlet oxygen formation mechanism is direct excitation of surface-absorbed oxygen (similar to metal oxides) [27]. More intense luminescence was observed when copper was exposed to UV light ( $\lambda = 365$  nm). Spectral dependence of singlet oxygen luminescence intensity with direct optical excitation is shown in Figure 5. The Figure shows the intensities in the oxygen luminescence spectrum profile peak ( $\lambda = 1270$  nm) assigned to the light flux density at the LED matrix outlet. The calculation of values shown in Figure 5

considered only the singlet oxygen phosphorescence signal observed above the background luminescence of copper surface.

Relatively low intensity of the singlet oxygen luminescence peak compared with copper surface luminescence intensity observed in Figure 4 is explained by the difference in copper particle concentration on the copper surface and concentration of oxygen molecules absorbed on this surface. Both molecular oxygen excitation mechanisms contribute to the observed singlet oxygen luminescence peak intensity: photocatalytic and direct optical excitation of oxygen molecules.

#### 4. Copper membrane air decontamination unit

Air decontamination unit was developed using the copper based photocatalytic element (microporous bronze membrane with a thickness of 3 mm and diameter of 150 mm). The microporous membrane used in the unit has pore sizes  $0.5\text{--}20\ \mu\text{m}$  that were selected to ensure sufficiently full penetration into the porous membrane structure of most pathogenic organisms present in air, e.g. influenza virus or coronavirus with an average size of  $0.1\ \mu\text{m}$ , and such pathogenic bacteria as staphylococci — about  $10\ \mu\text{m}$  or little more. High degree of microporous membrane structure branching combined with sufficient thickness ensure high-performance photocatalytic and contact activity of copper for air sterilization. It should be noted that such membrane has also rather high gas permeability: inactivated air flow rate range may be 100 to  $400\ \text{m}^3/\text{h}$  at linear flow rate 1.0 to 5.0 m/s.

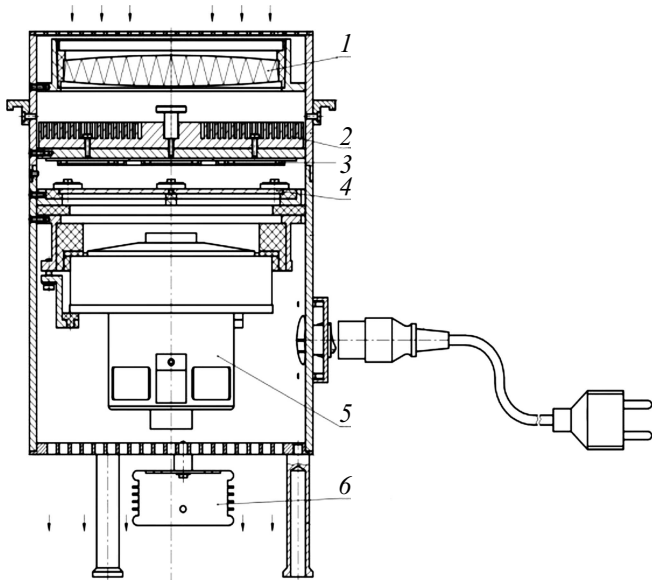


**Figure 6.** Air decontamination unit diagram: 1 — inlet filter, 2 — LED matrix cooling radiator, 3 — LED matrices, 4 — photocatalytic membrane, 5 — fan, 6 — LED matrix power supply.

The proposed photocatalytic air purification and sterilization method may be implemented using the unit (UOV-1) shown in Figure 6.

The unit operation sequence is as follows. Air is sucked into the air intake by fan 5, filtered by inlet filter 1 to remove dust and moisture, flows through the hole in radiator 2 which cools down LED matrices 3, and is delivered to photocatalytic membrane surface 4 illuminated by white light from ARPL-100W-EPA-5060 LED matrices.

The LEDs emitting in 400 to 780 nm visible spectrum ensure continuous illumination of photocatalytic element based on microporous copper or bronze membrane with white light with a flux density of at least  $250\text{--}500\ \text{mW}/\text{cm}^2$ . Total power consumption of the air purification unit is 1 kW. It is spent primarily to air flow purging through the microporous membrane.

Bacteria and viruses contained in the purified air are entrapped in the microporous membrane and inactivated under the action of contact with copper during „contact killing“ and interaction with reactive oxygen intermediates formed on the porous membrane surface exposed to LED light. The purified air at the microporous membrane outlet flow further through the fan holes and enters the room through the outlet hole.

Testing of the proposed air purification and sterilization unit using a photocatalytic porous bronze membrane exposed to LED light, through which the purified air is purged, was carried out in Smorodintsev Research Institute of Influenza (Saint Petersburg) in June 2020.

#### 5. Antiviral activity of copper-based photocatalytic element unit

Testing of the unit's virucidal activity (UOV-1 air decontamination unit) against flu influenza A virus, strain A/PR/8/34 (H1N1) was carried out using aspiration (aerosol) technique.

##### 5.1. Test systems

##### 5.1.1. Cell cultures

MDCK (Madin-Darby canine kidney) cell culture was received from the cell culture laboratory collection of „Smorodintsev Research Institute of Influenza“. During the testing, passage level after defrosting did not exceed 20 passages.

The cell suspension ( $10^5\ \text{cell}/\text{ml}$ ) was placed into 96-well plates and inoculated during 24 hours in  $\text{CO}_2$  incubator at  $37^\circ\text{C}$  and 5%  $\text{CO}_2$ , then monolayer density was assessed visually using inverted microscope. Only that plates where monolayer confluence was higher than 90% were selected for testing.

Virucidal efficiency of the tested instrument against the influenza A virus in air

Experiment №	Virus titer, lg TID <sub>50</sub> /0.2 ml			
	Without treatment	After treatment by UOV-1	Difference in titers compared with reference sample	Average titer differences
1	4.5	0	4.5	4.0 ± 0.5
2	4.0	0	4.0	
3	3.5	0	3.5	

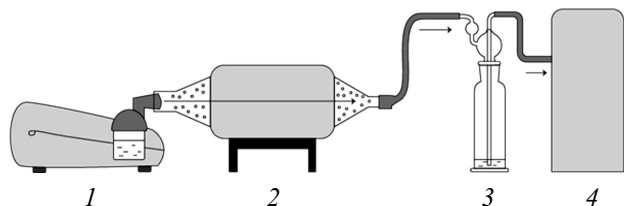


**Figure 7.** Aerosol setup for air decontamination performance testing using UOV-1: 1 — nebuliser, 2 — UOV-1, 3 — Drechsel bottle, 4 — aspirator.

### 5.1.2. Maintenance media

To 100 ml of DMEM medium (DMEM medium with glutamine, Biolut, Saint Peterburg), 1 ml of antibiotic solution (ciprofloxacin, Sintez, Kurgan) and 0.1 ml TPCK-trypsin solution (final concentration in 1 µg/ml medium) were added.

### 5.1.3. Viruses

Influenza A virus, strain A/PR/8/34 (H1N1) received from the working collection of the viral infection chemotherapy laboratory. The virus was expanded in allantoic cavity of 10-day embryonated hen's eggs, then allantoic liquid was collected from the eggs, clarified by centrifugation at 7000 rpm, and then the virus was concentrated by centrifugation at 20000 rpm. Viral sediment was resuspended in saline solution up to 10<sup>8</sup> lgTID<sub>50</sub>/0.1 ml and the obtained suspension was sprayed in aerosol chamber.

### 5.1.4. Aerosol system for air decontamination performance testing

Operations were carried out in sealed glove box which was used as aerosol chamber. Virus containing liquid was sprayed using Microlife NEB-10 medical nebuliser in mode № 3 (particle size 10–14 µm). Air was mixed with aerosol using Orient F2035 fan. 50 m<sup>3</sup> air samples were taken using PU-4E aspirator by passing culture fluid through Drechsel bottle.

Virus containing fluid was sprayed inside a sterile box by supplying virus aerosol from the nebuliser through the funnel into the instrument (as shown in Figure 7). The treated aerosol was collected at the instrument outlet through the

second funnel with passing through the Drechsel bottle filled with culture fluid. The reference samples were taken by the similar method using a hollow plastic vessel of an appropriate size instead of the instrument.

### 5.2. Virucidal efficiency assessment

The suspension containing influenza virus concentrate was sprayed and samples were taken as described above. Then virus titer in the samples was assessed as follows: a set of 10-fold dilutions (10<sup>-1</sup>–10<sup>-7</sup>) was prepared from samples on DMEM medium with glutamine, 20 µg/ml of ciprofloxacin was added, then 10-day embryonated hen's eggs were infected by them. The eggs were incubated during 72 h at 37°C.

Virus titer in allantoic liquid of each egg was tested using hemagglutination reaction for which 100 µl of allantoic liquid was transferred into the appropriate wells of immunology plates with U-shape bottom and equal volume of 1-% of hends erythrocyte suspension in saline solution was added. After 40 min, presence or absence of haemagglutination was tested visually. Virus titer was calculated using Reed and Muench method [28].

### 5.3. Virucidal efficiency of UOV-1

Virucidal activity test results of the air decontamination instrument test sample based on copper containing membrane (UOV-1) are presented in the table where TID<sub>50</sub> is 50-% tissue infectious dose — virus dose contaminating 50% of cells.

The table shows that the use of the tested instrument in each of the experiments caused full inactivation of infectious activity of influenza virus (virus titer = 0) lg TID<sub>50</sub>/0.2 ml, and the difference with the reference sample was 3.5 to 4.5 lg TID<sub>50</sub>/0.2 ml.

The obtained data was confirmed by RCR test: in test samples after treatment in UOV-1 influenza A virus was released at cycle 20.17, and in reference samples (without treatment in UOV-1) — at cycle 13.95.

### Conclusion

The paper contains the results of development of the air photocatalytic purification and sterilization method and de-

vice based on the use of two physical methods of destructive impact on bacteria and viruses based on oxidizing properties of photocatalysis, including singlet oxygen, and also on decontaminating properties of copper-based materials used in the device. In the developed device, the contaminated air flows through the catalytic microporous copper membrane illuminated with white light from LED matrices.

The proposed air decontamination method and device have no high voltages, air ozone treatment, and UV irradiation. As opposed to photocatalytic devices with titanium dioxide element, the proposed copper- and/or copper alloy based photocatalytic element has higher structural strength. This device uses not only a catalyst surface layer (as with titanium dioxide), but the whole membrane volume during contact destruction and photocatalytic mechanism due to deep light penetration into the membrane.

The virology testing has shown that the air sterilization device based on copper or copper alloy membranes results in full infectious inactivation of the influenza virus sprayed in the form of 10–14  $\mu\text{m}$  particles during aspiration test. Thus, the obtained data confirm that UOV-1 air decontamination unit is an effective device for influenza virus elimination in air environment.

The listed results were obtained on the influenza virus — representative of *Ofrthomyxoviridae* family. Viruses from this family are enveloped RNA genome viruses, i.e. have phospholipid capsule on virion surface, and genetic material of the virus is represented by RNA molecules. Most human viruses causing ARVI have the same configuration (RS virus, parainfluenza virus, coronaviruses, including SARS-CoV-2). According to this, these viruses are close to each other in terms of thermostability. Thus, despite the absence of experimental data on the efficiency of the described air purification method against each of the listed viruses, we can suppose with great probability that the remaining viruses from this list will be inactivated with the same efficiency using UOV-1. Other viruses causing ARVI and having no envelope (rhinoviruses and adenoviruses) are more thermoresistant and may require higher energy and/or longer exposition for full inactivation.

## Acknowledgments

The authors express thanks to D.A. Loiznov, doctor of medicine, Deputy Director of „Smorodintsev Research Institute of Influenza“ of the Ministry of Health of Russia, for the arrangement of virology testing of UOV-1, and „Smorodintsev Research Institute of Influenza“ personnel (A.V. Galochkina, Senior Associate, A.V. Garshinina, Research Fellow, G.S. Petukhova, Research Fellow, Yu.V. Nikolaeva, Junior Fellow) for participation in this testing.

The authors express thanks to A.N. Vasiliev and V.S. Pimchenko for th assistance in preparation of UOV-1 virology test sample, and „Safety Technologies“ — for financial support of sample preparation.

## Conflict of interest

The authors declare that they have no conflict of interest.

## References

- [1] R. Gasparini, D. Amicizia, L.P. Lai, N.L. Bragazzi, D. Panatto. *J. Prev. Med. Hyg.*, **55** (3), 69 (2014).
- [2] K. Rogers. 1968 flu pandemic. *Encyclopedia Britannica* [Electronic source] Available at: <https://www.britannica.com/event/1968-flu-pandemic>. (date of access 11.20.2021) 24.12.2021.
- [3] S. Rewar, D. Mirdha, P. Rewar. *Ann. Glob. Health*, **81** (5), 645 (2015). DOI: 10.1016/j.aogh.2015.08.014.
- [4] R.S. Dreizen, N.V. Astafieva. *Ostrye respiratornye zabolevaniya* (Meditsina, Moskva, 1991)
- [5] L.M. Vasilyak. *Uspekhi prikladnoi fiziki*, **6**(1), 5 (2018).(in Russian).
- [6] Hepa Filter: pat. 6428610 USA. Tsai R., Malkan S.R.; № US09/484864; zayavl. 18.01.2000; opubl. 06.08.2002.
- [7] *Ustroistvo dlya obezzaazhivaniya vozdukh*: pat. 2058156 Ros. Federatsiya (in Russian). Fokanov V.P., Pavlov A.B., Baboshin V.N., Shallar' A.V., Irgashev B.B.; № 93 93009355; zayavl. 17.02.1993; opubl. 20.06.2000, Byul. № 17.
- [8] M. Raeiszadeh, B. Adeli. *ACS Photonics*, **7** (11), 2941 (2020). DOI: 10.1021/acsp Photonics.0c01245.
- [9] *Ustroistvo dlya ochistki i obezzaazhivaniya vozdukh*: pat. 2033272 Ros. Federatsiya (in Russian). Pershin A.F., Baidukin Yu.A., Kazeev Yu.R., Fedorov A.V.; № 5031025/15; zayavl. 03.04.1992; opubl. 20.04.1995, Byul. № 24.
- [10] *SanPiN 1.2.3685-21 „Gigienicheskiye normativy i trebivaniya k obespecheniyu bezopasnosti i (ili) bezvrednosti dlya cheloveka faktorov sredy obitaniya“* (Tsentrimg, Moskva, 2022)
- [11] *Ustroistvo dlya sterilizatsii i tonkoi fil'tratsii gaza*: pat. 2026751 Ros. Federatsiya (in Russian). Volodina E.V., Nagolkin A.V.; № 5048011/26; zayavl. 13.05.1992; opubl. 20.01.1995.
- [12] A.O. Ibadon, P. Fitzpatrick. *Catalysts*, **3**, 189 (2013). DOI: 10.3390/catal3010189
- [13] Y. Nosaka, T. Daimon, A.Y. Nosaka, Y. Murakami. *Phys. Chem. Chem. Phys.*, **6**, 2917 (2004). DOI: 10.1039/B405084C
- [14] D.Yu. Semenov, Yu.L. Vasiliev, S.S. Dydykin, E.F. Stranadko, V.K. Shubin, Yu.K. Bogomazov, V.A. Morokhotov, A.N. Shcherbyuk, S.V. Morozov, Yu.I. Zakharov. *Biomed. Photon.*, **10** (1), 25 (2021). DOI: 10.24931/2413-9432-2021-10-1-25-31
- [15] P.C.V. Conrado, K.M. Sakita, G.S. Arita, C.B. Galinari, R.S. Gonçalves, L.D.G. Lopes, M.V.C. Lonardon, J.J.V. Teixeira, P.S. Bonfim-Mendonça, E.S. Kioshima. *Photodiagn. Photodyn.*, **34**, 102221 (2021). DOI: 10.1016/j.pdpdt.2021.102221
- [16] *Fotokataliticheskiy element dlya ochistki i obezazhivaniya vozdukh i body i sposob ego izgotovleniya*: pat. 2647839 Ros. Federatsiya (in Russian). Balikhin I.L., Berestenko V.I., Domashnev I.A., Kabachkov E.N., Kurkin E.N., Troitsky V.N.; № 2015123582; zayavl. 20.12.2012; opubl. 21.03.2018, Byul. № 9.

- [17] *Sposob ochistki vozdukha ot organicheskikh primesei*: pat. 2071816 Ros. Federatsiya (in Russian). Vargauzin A.A., Kuzmin G.N., Kurganov S.V., Spichkin G.L., Chistov E.K.; № 92 92010987; zayavl. 20.01.1997; opubl. 10.06.2002, Byul. № 16.
- [18] C. Rueda-Romero, G. Hernández-Pérez, P. Ramos-Godínez, I. Vázquez-López, R.O. Quintana-Belmares, E. Huerta-García, E. Stepien, R. López-Marure, A. Montiel-Dávalos, E. Alfaro-Moreno. *Part. Fibre Toxicol.*, **13**(1), 36 (2016). DOI: 10.1186/s12989-016-0147-3
- [19] J. Zhao, L. Bowman, X. Zhang, V. Vallyathan, S.-H. Young, V. Castranova, M. Ding. *J. Toxicol. Env. Heal. A*, **72**(19), 1141 (2009). DOI: 10.1080/15287390903091764
- [20] H. Jawad, A.R. Boccaccini, N.N. Ali, S.E. Harding. *Nanotoxicology*, **5**(3), 372 (2011). DOI: 10.3109/17435390.2010.516844
- [21] S.L. Warnes, Z.R. Little, C.W. Keevil. *mBio*, **6**(6), e01697 (2015). DOI: 10.1128/mBio.01697-15
- [22] *Sposob fotokatalicheskoy ochistki i sterilizatsii vozdukha*: pat. 2743705 Ros. Federatsiya (in Russian). Kiselev V.M., Belousova I.M., Bagrov I.V., Muraviova T.D., Starodubtsev A.M., Krus'ko T.K., Vasiliev A.N., Zarubaev V.V., Shtro A.A., Zhitenev O.S., Lioznov D.A., Pimchenko V.S.; № 2020129482; zayavl. 07.09.2020; opubl. 24.02.2021, Byul. № 6.
- [23] M. Vincent, R.E. Duval, P. Hartemann, M. Engels-Deutsch. *J. Appl. Microbiol.*, **124**, 1032 (2018). DOI: 10.1111/jam.13681
- [24] D. Mitra, E.-T. Kang, K.G. Neoh. *ACS Appl. Mater. Inter.*, **12**(19), 21152 (2020). DOI: 10.1021/acsami.9b17815
- [25] S.L. Warnes, C.W. Keevil. *PLOS One*, **8**(9), e75017 (2013). DOI: 10.1371/journal.pone.0098333
- [26] N.D. Khiavi, R. Katal, S.K. Eshkalak, S. Masudy-Panah, S. Ramakrishna, Hu Jiangyong. *Nanomaterials*, **9**(7), 1011 (2019). DOI: 10.3390/nano9071011
- [27] V.M. Kiselev, I.M. Kislyakov, A.N. Burchinov. *Opt. Spectr.*, **120**(4), 520 (2016). DOI: 10.1134/S0030400X16040123
- [28] L.J. Reed, H. Muench. *Am. J. Epidemiol.*, **27**, 493 (1938). DOI: 10.1093/oxfordjournals.aje.a118408